

Mechanical optimization of skateboard pumping

Florian Kogelbauer^{✉*}

Department of Mechanical and Process Engineering, ETH Zürich, Leonhardstrasse 27, 8092 Zürich, Switzerland

Shinsuke Koyama[†]

The Institute of Statistical Mathematics, Tokyo 190-8562, Japan

Daniel E. Callan[‡]

Brain Information Communication Research Laboratory Group, ATR Institute International, Kyoto 619-0288, Japan

Shigeru Shinomoto[§]

*Brain Information Communication Research Laboratory Group, ATR Institute International, Kyoto 619-0288, Japan;
Graduate School of Biostudies, Kyoto University, Kyoto 606-8501, Japan;
and Research Organization of Open Innovation and Collaboration, Ritsumeikan University, Osaka 567-8570, Japan*



(Received 28 December 2023; accepted 11 June 2024; published 5 August 2024)

Skateboarders perform a reciprocating motion on a curved ramp, called pumping, by moving their bodies up and down perpendicular to the ramp surface. We propose a simple mechanical model for this pumping motion and solve the equation of motion explicitly in angular coordinates. This allows us to derive an optimal control strategy to maximize amplitude by dynamically adjusting the center of mass of the skateboarder. This optimal strategy is compared to experimental results for the motion of a skilled and an unskilled skateboarder in a half-pipe, validating that a skilled skateboarder follows the optimal control strategy more closely.

DOI: [10.1103/PhysRevResearch.6.033132](https://doi.org/10.1103/PhysRevResearch.6.033132)

I. INTRODUCTION

Gaining popularity as an action sport in the early sixties, skateboarding grew into a social phenomenon that was even included as an official discipline in the 2021 Olympic Games [1]. From a scientific point of view, the mechanics of skateboarding have served as a versatile playground in classical dynamics and control theory [2,3]. Recently, skateboarding has also become popular as an appealing model problem from dynamic control in robotics [4–6]. Mimicking the delicate motion of human bodies during various dynamically involved actions, state-of-the-art machine learning techniques are applied to capture performance data [7]. We also refer to [8–10] for various in-depth considerations on the mechanics of the dynamics of skateboarding.

In this paper, we propose a different, bottom-up approach towards the optimal control of skateboarding by focusing on a particular confined motion with few degrees

of freedom as a test case: pumping on a ramp. Despite its utmost simplicity, our minimal model is consistent with experimental data we obtained from comparing the performance of a skilled and an unskilled skateboarder. This approach not only avoids the computational complexity that goes along with high-dimensional, multi-degree-of-freedom models but is also in tune with reduced-order modeling and nonlinear normal modes [11]. Indeed, the theory of nonlinear normal modes [12], i.e., the reduction to few effective degrees of freedom, is highly relevant in control problems [13] for mechanical systems. Apart from the appeal of a completely soluble, experimentally consistent example, our insights might prove useful as a basic test case for robotics as well [14].

II. MODELLING SKATEBOARD PUMPING

We aim to model the reciprocating, pumping motion of a skateboarder in the half-pipe. To this end, we propose a simple mechanical skateboarder model on a cylindrical ramp by analogy to the pumping motion on a swing, see Fig. 1, which is itself classically modeled as a variable-length pendulum [15,16]. The results obtained for the cylindrical ramp are then extended to the optimal control motion in the half-pipe by interpolating along the flat part of the ramp. The equation of motion for a frictionless variable-length pendulum takes the form [17]

$$(L - h)\ddot{\theta} - 2\dot{h}\dot{\theta} + g \sin \theta = 0, \quad (1)$$

*Contact author: floriank@ethz.ch

†Contact author: skoyama@ism.ac.jp

‡Contact author: dcallan@atr.jp

§Contact author: shigerushinomoto@gmail.com

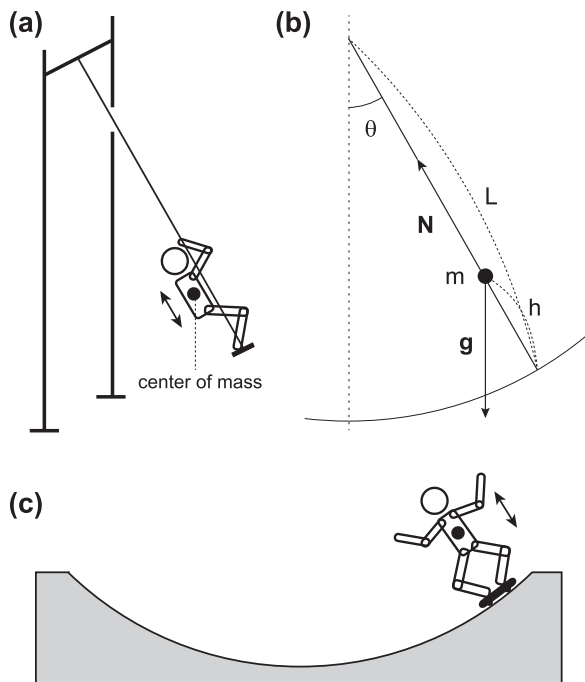


FIG. 1. Analogy of pumping motions. (a) Pumping on a swing. (b) The variable-length pendulum. (c) Pumping of a skateboarder on a cylindrical ramp.

where θ is the angle relative to a vertical axis, L is the radius of the cylindrical ramp, h is the height of the center of mass, and $g \sin \theta$ is the gravitational restoring force. A skateboarder controls his/her center of mass with respect to height, $h = h(t)$, perpendicular to the surface of the ramp. For more details on the dynamics of swinging, we refer to recent papers on the pumping of a swing taking into account the detailed aspects of swinging specific to human body movement [18–21]. The mechanism of height increase and gain in rotational motion is related to the conservation of angular momentum in the absence of friction. We therefore regard the height as an external control function to be optimised for maximal amplitude gain under certain constraints. Firstly, we assume that the height is constrained between a minimal bending and a maximal standing posture, $H_0 \leq h \leq H_1$. Secondly, we assume that the energy input through the muscular activity of the human or the control force of a skateboarding robot is limited, leading to a constraint in the acceleration of the height $|\dot{h}| \leq g$.

We consider Eq. (1) together with kinetic friction by assuming that the wheels of the skateboard kinetic friction μN at the surface of the ramp, where μ is a material-specific friction coefficient and N is the normal force

$$N = m(g \cos \theta + \ddot{h} + (L - h)\dot{\theta}^2). \quad (2)$$

The force term (2) results from balancing the force component normal to the ramp with gravity in the radial direction since $m(L - h)\dot{\theta}^2$ represents the centrifugal force.

Starting from an initial angle θ_0 and zero initial velocity $\dot{\theta}_0 = 0$, the height h is adjusted during a roll from the initial angle to the final angle θ^* at which all kinetic energy is consumed and the amplitude is maximal. Different height variations then lead to different maximal amplitudes θ^* . We

are interested in an optimal control function $\hat{h} = \hat{h}(t)$ such that

$$\hat{h}(t) = \arg \max_{\{h(t)\}} \theta^*[h(t)], \quad (3)$$

subject to the constraint $H_0 \leq h(t) \leq H_1$ and $|\dot{h}(t)| \leq g$ for all times. Problem (3) of controlling a variable-length pendulum under different constraints and damping mechanics has been considered in, e.g., [22,23]. To tackle the optimization problem (3) directly, we assume that the height is a monotonic function of time for a one-directional roll along the cylindrical ramp. Since the angle $\theta(t)$ along one roll is a monotonic function of time as well, we may rewrite the governing equation for the radius $r(\theta) = L - h(t)$ as a function of the angle, which will simplify the notation in the following. This allows us to derive an equation for the kinetic energy with respect to angular rotation $E_{\text{kin}} = \dot{\theta}^2/2$ as a function of θ .

Writing the kinetic energy and the radius as functions of the angle—the original dynamical variable—is reminiscent of the modern solution of the brachistochrone problem [24] and similar problems in the calculus of variations, thus leading to $E'_{\text{kin}} \equiv dE_{\text{kin}}/d\theta = \dot{\theta}$. By transforming the time derivative \dot{h} into the spatial derivative as $\dot{h} = -\dot{r} = -r'\dot{\theta}$, where $r' \equiv dr/d\theta$, the second-order differential equation in time (1) can be transformed into an analytically solvable first-order differential equation in angular coordinates,

$$rE'_{\text{kin}} + 4r'E_{\text{kin}} + g \sin \theta = 0. \quad (4)$$

Since the acceleration \ddot{r} can be transformed as $\ddot{r} = d/dt(r'\dot{\theta}) = \dot{\theta}r'' + \dot{\theta}^2r''$, we obtain a first-order differential equation for the kinetic energy E_{kin} with respect to θ for (2) as well,

$$rE'_{\text{kin}} + 4r'E_{\text{kin}} + g \sin \theta + \mu(g \cos \theta - r'E'_{\text{kin}} + 2(r - r'')E_{\text{kin}}) = 0. \quad (5)$$

The linear first-order differential Eq. (5) can be integrated easily to

$$E_{\text{kin}}(\theta) = -g \int_{\theta_0}^{\theta} \frac{\sin u + \mu \cos u}{r(u) - \mu r'(u)} \exp\left(\int_u^{\theta} f(s) ds\right) du, \quad (6)$$

$$f(s) = -\frac{4r'(s) + 2\mu(r(s) - r''(s))}{r(s) - \mu r'(s)}.$$

We remark that the influence of an air drag or an inertial drag proportional to the square of the velocity $F_{\text{air}} = C_D |\mathbf{v}| \mathbf{v}$ can be treated analogously to kinetic friction and an explicit formula similar to (6) may be derived by explicitly solving a linear differential equation for the angular kinetic energy. The numerical results for the optimal control strategy, however, show little deviation as compared to pure kinetic friction and we focus on formula (6) henceforth. At the maximal amplitude θ^* along one monotonic roll, all kinetic energy is consumed and we have that $E_{\text{kin}}(\theta^*) = 0$. Setting $\mu = 0$ in (6) we immediately see that the optimal control strategy in the frictionless case is given by

$$\hat{r}_{\text{frictionless}}(\theta) = \begin{cases} L - H_0, & (\theta_0 \leq \theta \leq 0), \\ L - H_1, & (0 < \theta), \end{cases} \quad (7)$$

where we have assumed that the skateboarder starts his/her roll on the left side of the ramp ($\theta_0 < 0$). The maximal angle

$\theta_{\text{frictionless}}^*$ achieved by this optimal control can be calculated explicitly as well and is given by

$$\cos \theta_{\text{frictionless}}^* = 1 - \left(\frac{L - H_0}{L - H_1} \right)^3 (1 - \cos \theta_0). \quad (8)$$

Solutions (7) and (8) will serve as a benchmark for the full, physically meaningful optimal control with constraints.

III. OPTIMIZATION PROBLEM AND NUMERICAL SOLUTION

As potential pumping strategies, we examine a two-parameter family of logistic functions interpolating between maximal and minimal height,

$$r(\theta) = L - H_0 - \frac{H_1 - H_0}{1 + e^{-\beta(\theta - \delta)}}, \quad (9)$$

for the pumping momentum β and the timing parameter δ . For the numerical simulation, we choose a friction coefficient of $\mu = 0.02$, which is consistent with the experimentally obtained coefficient. We compare the optimal pumping strategies for the cylindrical parts of the half-pipe in Fig. 2 for the frictionless case, unbounded acceleration, acceleration bounded by $|\ddot{h}| \leq g$, and unsuccessful pumping motions, where the achieved maximal angle θ^* is smaller than the initial amplitude $|\theta_0|$.

We continue with the analysis of the full half-pipe, starting with an initial position of the skateboarder at the left cylindrical part of the ramp ($\theta_0 < 0$). To enter the flat zone linking the two cylindrical parts with the highest possible speed, we seek optimal parameters β and δ from (9) such that E_{kin} is maximal at $\theta = 0$ (entering the flat zone). During the motion in the flat zone, the height h is decreased to H_0 continuously until leaving the flat zone again. Upon entering the right cylindrical part, we search for another set of parameters in (9) so that the final angle of a skateboarder θ^* is maximized. Similar to the cylindrical ramp, we note that in the frictionless case, the maximal amplitude can be calculated explicitly to

$$\cos \theta^* = 1 - \left(\frac{L - H_0}{L - H_1} \right)^5 (1 - \cos \theta_0). \quad (10)$$

We remark that the maximal angle is larger than the one of the cylindrical ramp (8) since the skateboarder performed two pumping cycles in the half-pipe. Figure 3 compares the optimal pumping strategies in the half-pipe for bounded acceleration (thick-blue line), the frictionless case (solid-black line), the case with friction but acceleration unbounded (dashed-green line), and two examples of unsuccessful pumping (brown- and orange-dotted lines) where the achieved maximal angle is smaller than the initial amplitude.

Here, we have chosen a friction coefficient of $\mu = 0.02$ and an initial angle of $\theta_0 = -1.3$ to be consistent with the experimental conditions described below.

IV. EXPERIMENTAL VALIDATION

To experimentally validate the optimal control strategy, we requested two skateboarders of different skill levels to gain as much height (or angle achieved) as possible by using their most efficient pumping action. The skilled skateboarder has

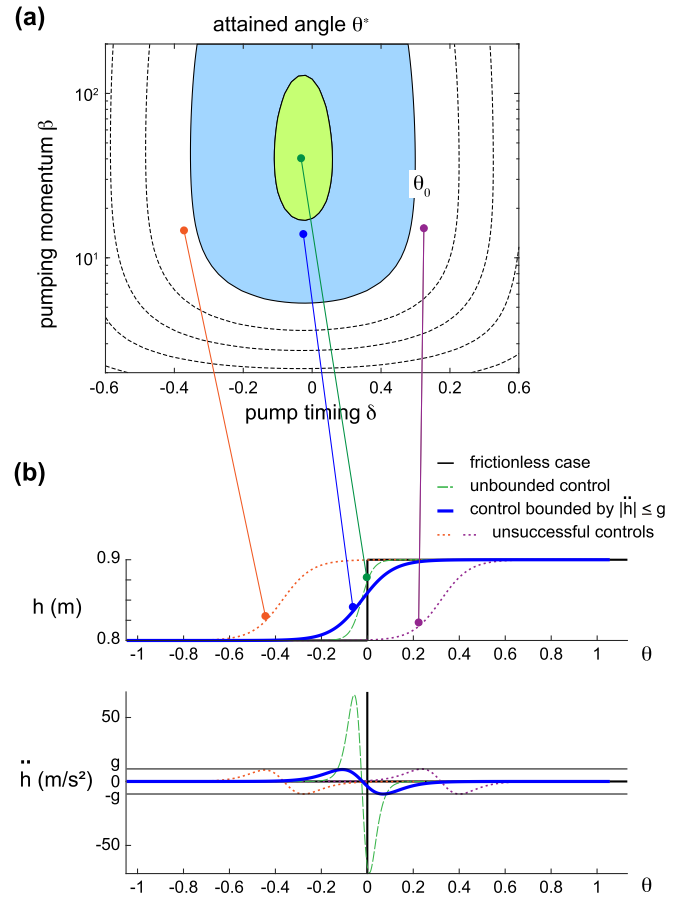


FIG. 2. Pumping on a cylindrical ramp in the presence of kinetic friction. (a) The attained angle θ^* plotted against the pumping timing δ and pumping momentum β . (b) The optimal height h and its acceleration \ddot{h} in the frictionless case (solid-black line); unbounded control in the presence of kinetic friction (green-dashed line); and the optimal solution under the acceleration bounded by $|\ddot{h}| \leq g$ (thick-blue line). The optimal strategies for a cylindrical ramp are compared with unsuccessful controls where an achieved angle θ^* is smaller than the initial angle $|\theta_0|$ (brown- and orange-dotted lines). Parameters: $\theta_0 = -\pi/3$, $L = 3$, $H_0 = 0.8$, $H_1 = 0.9$, and $\mu = 0.02$.

eleven years of experience, while the unskilled skateboarder has two years of experience. For each trial, they started from a position of rest and stopped their pumping when they reached the top of the ramp. The subject's center of mass was estimated automatically by the motion-capture software Xsens. The motion-capture (MOCAP) of the skateboarder was accomplished by the Xsens wireless system using 17 inertial measurement units (IMUs) placed on various segments of the entire body (feet, lower legs, upper legs, hands, fore arms, upper arms, shoulders, pelvis, sternum, and head). The sampling rate was 60 Hz. The spatial localization of the Xsens MOCAP is facilitated by utilizing four Vive IR Base stations and five trackers located on the lower legs, forearms, and pelvis. The Xsens MVN Analyze software was used to integrate Xsens and Vive tracking to produce full body kinematic data including joint angles, segment orientations, and center of mass as well as position. The acceleration in the sagittal plane $\{a_x, a_y\}$ was translated into the height acceleration measured relative

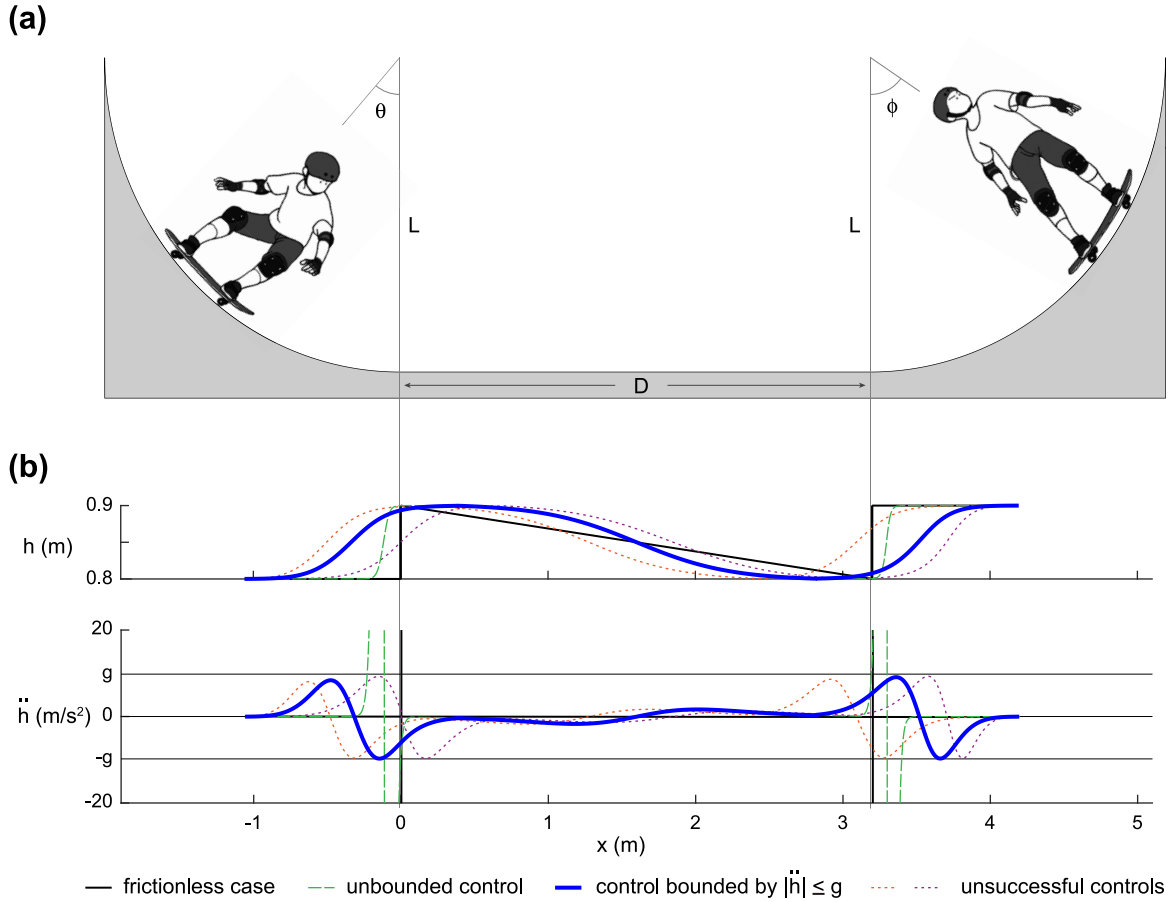


FIG. 3. (a) Simulations for the optimal pumping motion of a skateboarder on a half-pipe consisting of two cylindrical ramps connected by a flat zone in between. The radius of curvature of the cylindrical parts is $L = 1.9$ m and the width of the flat zone is $D = 3.2$ m, corresponding to the experimental conditions. (b) Height and acceleration for different pumping strategies: optimal control for the frictionless case (black line), optimal unbounded control in the presence of kinetic friction (dashed green line), and optimal control under the acceleration bounded by $|\ddot{h}| \leq g$ (blue thick line). The optimal controls are compared with unsuccessful pumping (brown and orange dotted lines), where the maximal angle achieved is less than the initial amplitude. Parameters: $\theta_0 = -1.3$, $H_0 = 0.8$, $H_1 = 0.9$, and $\mu = 0.02$.

to the ramp surface \ddot{h} using information about the center of mass of the subjects.

Figure 4(a) shows snapshots of the skilled and unskilled skateboarders performing reciprocating during the experiment. Figures 4(b)–4(d) show their horizontal velocity v_x and vertical velocity v_y as well as the acceleration \ddot{h} . Each black-solid curve represents a left-to-right motion segmented from the back-and-forth motion.

Firstly, the friction coefficient μ is estimated from the decrease in horizontal velocity in Fig. 4(b). With an average speed of $v \approx 3$ m/s, the skateboarder took $\Delta t \approx 1$ s to pass the flat zone of 3 m. The velocity decreased by $\Delta v \approx 0.2$ m/s during this passage, implying that the change in velocity $\Delta v / \Delta t = \mu g$ or $\mu \approx 0.02$. We also used this friction coefficient as an input parameter for the theoretical estimation described above.

Secondly, we have compared the estimated acceleration with the optimal acceleration obtained by our theory [Fig. 3(b)]. The skilled skateboarder had a smaller root-mean-square error (3.8 m/s²) with the theoretical optimal solution than the unskilled skateboarder (4.3 m/s²). This indicates that our theoretical-numerical optimal pumping strategy is

followed more closely by the skilled skateboarder as compared to the unskilled one. We emphasize that our theory is suggesting a more efficient motion even for the skilled skateboarder.

V. CONCLUSIONS

We conclude with a summary of the results. We modeled the pumping motion of a skateboarder in a half-pipe as a variable-length pendulum with kinetic friction in the cylindrical part of the ramp surface and solved the equation of motion explicitly for the kinetic energy in angular coordinates. This allows us to formulate an optimization problem for the maximal angle in one roll. The results were compared to an experimental study in which the pumping strategies of skilled and unskilled skateboarders trying to gain height were compared. The skilled skateboarder showed less deviation from the theoretically predicted optimal control strategy.

We have shown that a simple mechanical model can accurately represent specific aspects of the highly complex and delicate motion of skateboarding and may even suggest potential improvements in an athlete's performance. This type

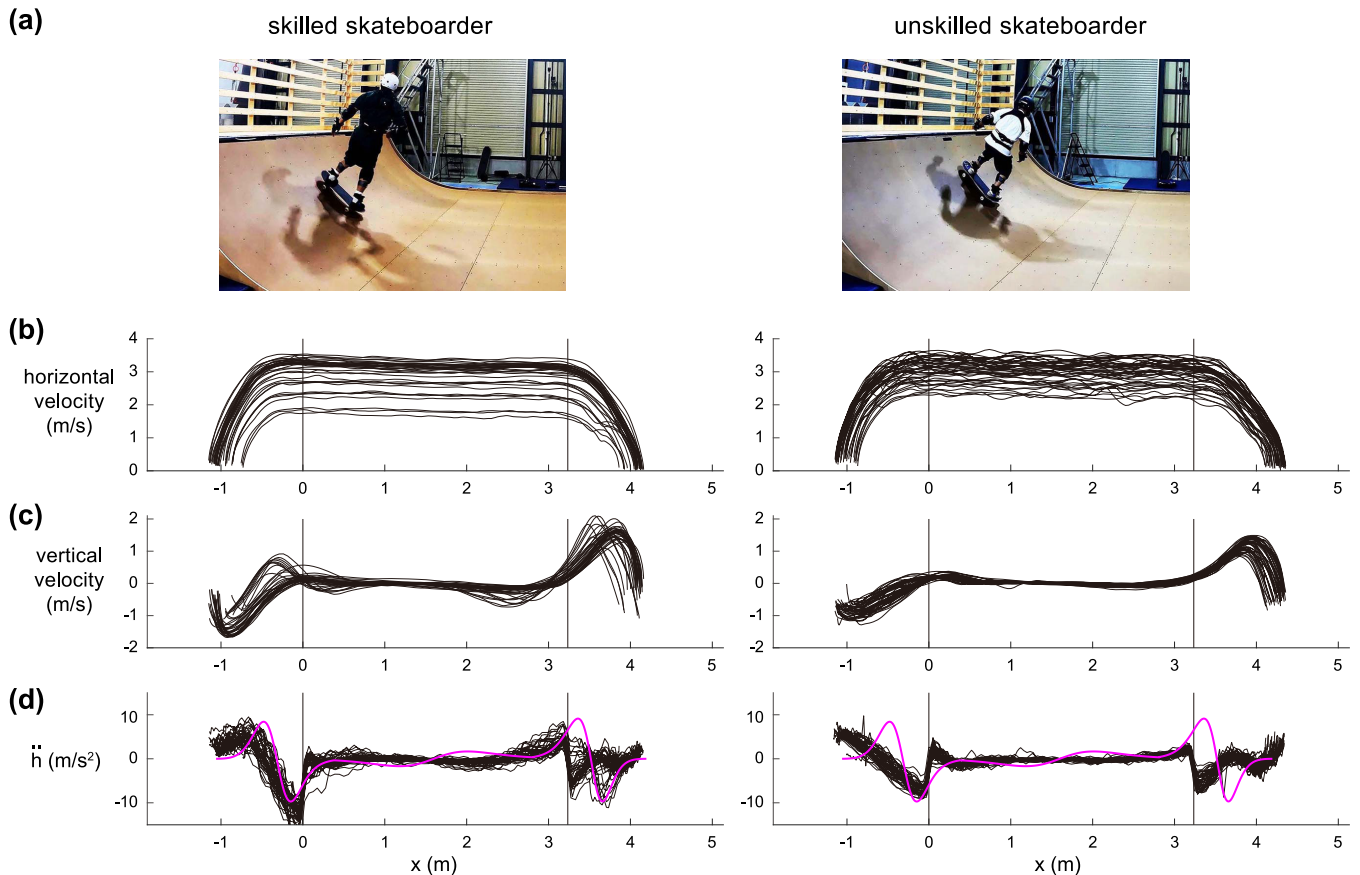


FIG. 4. (a) Pumping on a half pipe performed by skilled and unskilled skateboarders. (b) and (c) The horizontal and vertical velocities of the center of mass. Each line represents a left-to-right motion segmented from the back-and-forth motion. (d) The acceleration of the height from the ramp surface, \ddot{h} . The magenta line shows the theoretical-numerical prediction of the optimal control strategy.

of kinematic consideration on a simplified low-degree-of-freedom model could also be used to investigate improved motions in other sports, such as ski jumping. The presented model might be extended to include other degrees of freedom, such as lateral motion or rigid body properties.

ACKNOWLEDGMENTS

We thank K. Tsuchiya, E. Uchibe, and S. Takagi for constructive comments, and K. Shinomoto for drawing the

illustrations for Fig. 3. D.E.C. and S.S. were supported by the New Energy and Industrial Technology Development Organization (NEDO). S.S. was supported in part by the Japan Society for the Promotion of Science (JSPS) KAKENHI No. 22H05163.

F.K. and S.K. contributed equally to this work. F.K. developed the analytical method and wrote the paper. S.K. performed the optimization and numerical analysis. D.E.C. performed the experiments. S.S. designed the study and drafted the manuscript.

- [1] T. Hawk, *The A to Z of Skateboarding* (Unbound Publishing, London, 2019).
- [2] B. Varszegi, D. Takacs, and G. Stepan, Skateboard: A human controlled non-holonomic system, in *Proceedings of the 11th International Conference on Multibody Systems, Non-linear Dynamics, and Control* (ASME, Boston, MA, 2015), Vol. 6, pp. 1–6.
- [3] B. Varszegi, D. Takacs, G. Stepan, and S. J. Hogan, Stabilizing skateboard speed-wobble with reflex delay, *J. R. Soc. Interface* **13**, 20160345 (2016).
- [4] K. Kim, P. Spieler, E.-S. Lupu, A. Ramezani, and S.-J. Chung, A bipedal walking robot that can fly, slackline, and skateboard, *Sci. Robot.* **6**, eabf8136 (2021).
- [5] S. Ito, S. Sugiura, Y. Masuda, S. Nohara, and R. Morita, Mechanism and control of a one-actuator mobile robot incorporating a torque limiter, *J. Intell. Robot. Syst.* **97**, 431 (2020).
- [6] S. Iannitti and K. M. Lynch, Minimum control-switch motions for the snakeboard: A case study in kinematically controllable underactuated systems, *IEEE Trans. Robot.* **20**, 994 (2004).

- [7] Google Skate Project, https://about.google/intl/ALL_au/stories/project-skate/, accessed: 2023-12-15.
- [8] A. S. Kuleshov, Various schemes of the skateboard control, *Procedia Eng.* **2**, 3343 (2010).
- [9] Z. C. Feng and M. Xin, Energy pumping analysis of skating motion in a half pipe and on a level surface, *Eur. J. Phys.* **36**, 015002 (2015).
- [10] M. Hubbard, Human control of the skateboard, *J. Biomech.* **13**, 745 (1980).
- [11] G. Kerschen, M. Peeters, J. C. Golinval, and A. F. Vakakis, Nonlinear normal modes, Part I: A useful framework for the structural dynamicist, *Mech. Syst. Signal Process.* **23**, 170 (2009).
- [12] G. Haller and S. Ponsioen, Nonlinear normal modes and spectral submanifolds: existence, uniqueness and use in model reduction, *Nonlinear Dyn.* **86**, 1493 (2016).
- [13] M. Peeters, R. Vigiú, G. Sérandour, G. Kerschen, and J.-C. Golinval, Nonlinear normal modes, Part II: Toward a practical computation using numerical continuation techniques, *Mech. Syst. Signal Process.* **23**, 195 (2009).
- [14] S. Syed, Motion planning for skateboard-like robots in dynamic environments, *XRDS: Crossroads, The ACM Magazine for Students* **15**, 3 (2008).
- [15] P. L. Tea, Jr. and H. Falk, Pumping on a swing, *Am. J. Phys.* **36**, 1165 (1968).
- [16] J. A. Burns, More on pumping a swing, *Am. J. Phys.* **38**, 920 (1970).
- [17] S. Shinomoto and H. Sakaguchi, in *Mechanics*, edited by T. Uematsu, H. Aoyama, and T. Maskawa (Tokyo Tosho, Tokyo, 2013).
- [18] L. A. Klimina and A. M. Formalskii, Three-link mechanism as a model of a person on a swing, *J. Comput. Syst. Sci. Int.* **59**, 728 (2020).
- [19] P. Glendinning, Adaptive resonance and pumping a swing, *Eur. J. Phys.* **41**, 025006 (2020).
- [20] S. Koshkin and V. Jovanovic, Swinging a playground swing: Torque controls for inducing sustained oscillations, *IEEE Control Syst.* **42**, 18 (2022).
- [21] C. Hirata, S. Kitahara, Y. Yamamoto, K. Gohara, and M. J. Richardson, Initial phase and frequency modulations of pumping a playground swing, *Phys. Rev. E* **107**, 044203 (2023).
- [22] M. Anderle, P. Appeltans, S. Čelikovský, W. Michiels, and T. Vyhřídál, Controlling the variable length pendulum: Analysis and Lyapunov based design methods, *J. Franklin Inst.* **359**, 1382 (2022).
- [23] E. K. Lavrovskii and A. M. Formal'skii, Optimal control of the pumping and damping of a swing, *J. Appl. Math. Mech.* **57**, 311 (1993).
- [24] H. Erlichson, Johann Bernoulli's brachistochrone solution using Fermat's principle of least time, *Eur. J. Phys.* **20**, 299 (1999).